Lung exposure to nanoparticles modulates an asthmatic response in a mouse model of asthma

*Salik Hussain[1,2], *Jeroen AJ Vanoirbeek[2], Katrien Luyts[2], Vanessa De Vooght[2], Erik Verbeken[3], Leen CJ Thomassen[4], Johan A Martens[4], David Dinsdale[5], Sonja Boland[1], Francelyne Marano[1], Benoit Nemery[2], Peter HM Hoet[2]

* First two authors equally contributed to this manuscript

Affiliations

[1] Unit of Functional and adaptive Biology (BFA) CNRS EAC 4413, Laboratory of Molecular and Cellular Responses to Xenobiotics, Univ. Paris Diderot, Paris, France.

[2] Research Unit for Lung Toxicology, K.U.Leuven, Leuven, Belgium.

[3] Morphology and Molecular Pathology Section, K.U.Leuven, Leuven, Belgium

[4] Center for Surface Chemistry & Catalysis, K.U.Leuven, Heverlee, Belgium.

[5] MRC Toxicology Unit, University of Leicester, Leicester, UK

Running title: Nanoparticles aggravate diisocyanate-induced asthma

Corresponding Author

Prof. Peter HM Hoet

K.U.Leuven

Department of Occupational, Environmental and Insurance Medicine

Research Unit for Lung Toxicology

Herestraat 49 bus 706

3000 Leuven

Belgium

Tel: +32 16 33 01 97

Fax: +32 16 34 71 24

E-mail: peter.hoet@med.kuleuven.be

Abstract

The aim of this study was to investigate the modulation of an asthmatic response by titanium dioxide (TiO_2) or gold (Au) nanoparticles (NPs) in a murine model of diisocyanate-induced asthma.

On days 1 and 8, BALB/c mice received 0.3% toluene diisocyanate (TDI) or the vehicle acetone-olive oil (AOO) on the dorsum of both ears (20 µl). On day 14, the mice were oropharyngeally dosed with 40 µl of a NP suspension (0.4 mg/ml ~ 0.8 mg/kg TiO_2 or Au). One day later (day 15), the mice received an oropharyngeal challenge with 0.01%TDI (20 µl). On day 16, airway hyperreactivity (AHR), bronchoalveolar lavage (BAL) cell and cytokine analysis, lung histology and total serum IgE were assessed.

NP exposure in sensitized mice led to a 2-fold (TiO_2) and 3-fold (AU) increase in AHR, and a 3-fold or 5-fold increase in BAL total cell counts, mainly comprising neutrophils and macrophages. The NPs taken up by BAL macrophages were identified by energy dispersive X-ray spectroscopy (EDX). Histological analysis revealed increased oedema, epithelial damage and inflammation.

In conclusion, these results show that a low, intrapulmonary, dose TiO_2 or Au NPs can aggravate pulmonary inflammation and AHR in a mouse model of diisocyanate-induced asthma.

Keywords

Introduction

Occupational asthma accounts for an important percentage of work related respiratory illnesses [1]. It has been reported that at least 9-15% cases of asthma in adults are due to occupational exposures [2]. Isocyanates are widely used in various industrial and consumers products and they are a major cause of chemical-induced occupational asthma throughout the world [3].

We have previously described a mouse model of chemical-induced asthma using toluene diisocyanate (TDI) as sensitizing agent [4-6]. In this mouse model we initiate sensitization via dermal application, which is followed by a single airway challenge, resulting in asthma-like responses. In OA it is generally assumed that exposure to the respiratory tract is the key route and site for the initiation of the immune responses. However, despite reductions in workplace respiratory exposures, isocyanate asthma continues to occur, and this has prompted a focus on skin as a route of exposure [3;7-9]. Recently, several animal models have shown convincingly that skin exposure to chemical sensitizers (predominantly isocyanates, but also anhydrides and persulfate salts) can induce systemic sensitization, which may result in asthma-like respiratory responses when the animal is later challenged via the airways [5;10-12].

.

Current estimations indicate that more than 800 nanomaterials containing products are commercially available (Woodrow Wilson Database) [13]. These nanomaterials can affect health through consumer products as through well as occupational and environmental exposures [14;15]. Both titanium dioxide (TiO_2) and gold (Au) NPs are produced and used in substantial quantities and pose an emergent occupational and consumer risk [13]. Nanoparticles of titanium dioxide (TiO_2) are one of the most abundantly produced and widely utilized nanomaterials [16] with applications in sunscreens, cosmetics, tooth pastes, and food products [17;18]. The biological applications of gold NPs have been recently reviewed [19]. Gold NPs are medicinally used as drug delivery agents [20], in the treatment of rheumatoid arthritis [21], for photodynamic therapy of cancer [22] and as antimicrobial agents [23].

Modulation of pulmonary illnesses by a variety of occupational and environmental factors has been a topic of interest in the recent past. Previous knowledge of air pollution studies confirm the role of ultrafine particles (nanoparticles; NPs) in aggravating pulmonary illnesses [24]. A correlation between the use of asthma medication - linked to lung function disturbances - with environmental ultrafine particle exposure has been reported [25]. Indeed, different types of engineered NPs have been shown to induce pulmonary inflammation in experimental animals [26;27] as well as in cell lines of respiratory origin *in vitro* [28-31].

We hypothised that, in concordance to environmental PM, engineered NPs will enhance the inflammatory response in asthmatic subjects. In the present study we investigated the modulation of airway hyperreactivity and inflammatory response by TiO_2 or Au in a mouse model of diisocyanate-induced asthma.

Materials and Methods

Nanoparticles (NP)

TiO$_2$ NPs (99.9% anatase) of 15nm primary particle size were obtained from Sigma-Aldrich (Saint Quentin Fallavier, France). Au NPs of 40 nm primary particle size were prepared in the laboratory (Institut d'Electronique Fondamentale UMR CNRS 8622, Universite Paris-Sud, 91405 Orsay, France) by Turkevich method. Briefly, an aqueous solution of gold tetrachloroauric acid (82.8 mg of gold) was heated until boiling under vigorous stirring. Then, an aliquot of a 1% trisodium citrate aqueous solution was added and solution was then stirred and kept at boiling conditions for another 45 minutes. Au NPs with average sizes of 40 nm were prepared by adjusting the ratio [AuCl-4 Citrate] from 0.4 to 1.3. After the introduction of the citrate solution, a purple color appeared which then turned to ruby red. The solution was then stirred and kept at boiling conditions for another 45 minutes to complete the reduction process.

In all experiments NP suspensions (0.04 µg/mL) stabilized in 2.5 mM trisodium Citrate Tribasic dehydrate (Vehicle) (Sigma-Aldrich, Steinheim, Germany) were utilized to treat the mice.

Nanoparticle characterization

NPs were thoroughly characterized for their purity, hydrodynamic diameters, zeta potentials, spectral characteristics, electrophoretic mobility, and transmission electron microscopic analysis (TEM) (primary particle diameter and behavior in solution form).

Transmission Electron Microscopy (TEM)

Transmission Electron Microscopic (TEM) measurements were performed using a Philips CM30 TEM operating at 300 kV. Small volumes of sample (same concentration of NPs which was used to expose the mice, dissolved in trisodium citrate) were deposited on copper mesh grids and covered with carbon coating films. The samples were then dried under an N$_2$ atmosphere in a glove box.

Dynamic Light Scattering

Au and TiO$_2$ NPs were diluted to concentrations of 40 and 8 mg/L, respectively, in 2.5 mM trisodium citrate solution followed by ultrasonic treatment to reduce agglomeration. Homogeneous suspensions were obtained. Dynamic light

scattering measurements were performed with a Brookhaven 90 Plus (scattering angle: 90°, wavelength: 659 nm, power 15 mW). Correlation functions were analyzed with the Clementine package (maximum entropy method) for Igor Pro 6.02A. This resulted in intensity weighted distribution functions versus decay times. By converting the decay times with instrument parameters and physical parameters to hydrodynamic diameters, an intensity weighted size distribution is obtained. A lognormal fit was applied on each population resulting in the intensity weighed average hydrodynamic diameter of the population. Note that the hydrodynamic diameter is the kinetic unit comprising the bare particles and a solvation layer. It is a value that refers to how fast a particle diffuses within a fluid. It corresponds to the diameter of a sphere that has the same translational diffusion coefficient as the particle. Mass and number weighed distributions were estimated using the Rayleigh scattering approximation and a correction factor for the form factor of spherical particles [32].

Zeta Potential Measurements

Zeta potential measurements were performed on the same NP solutions as used for DLS. Au and TiO_2 NPs were diluted to concentrations of 40 and 8 mg/l, respectively, in 2.5 mM trisodium citrate solution (pH = 6.95, ionic strength I = 15 mM). Zeta potential was measured with a Brookhaven 90Plus/ZetaPlus instrument applying electrophoretic light scattering. A primary and reference beam (659 nm, 35 mW), modulated optics and a dip-in electrode system were used. The frequency shift of scattered light (relative to the reference beam) from a charged particle moving in an electric field is related to the electrophoretic mobility of the particle. The Smoluchowski limit was used to calculate the zeta potential from the electrophoretic mobility.

Reagents

Toluene-2,4-diisocyanate (TDI) (98%) (Fluka, CAS 584-84-9), acetyl-β-methylcholine (methacholine) and acetone were obtained from Sigma Aldrich (Bornem, Belgium). Pentobarbital (Nembutal) was obtained from Sanofi Santé animale (CEVA, Brussels, Belgium) and Isoflurane (Forene®) from Abbott Laboratories (S.A. Abbott N.V., Ottignies, Belgium). The vehicle (AOO) used to dissolve TDI consisted of a mixture of two volumes of acetone (A) and three volumes of olive oil (OO) ('extra virgin', Carbonell, Spain) for the dermal sensitization, and one

volume of acetone and four volumes of olive oil for the challenge. Concentrations of TDI are given as percent (v/v) in AOO.

Animals

Male BALB/c mice (approximately 20 g, 6 weeks old) were obtained from Harlan (the Netherlands). The mice were housed in a conventional animal house with 12h dark/light cycles. They received lightly acidified water and pelleted food (Trouw Nutrition, Gent, Belgium) ad libitum. All experimental procedures were approved by the local Ethical Committee for Animal Experiments.

Experimental Protocol

On days 1 and 8, mice were dermally sensitized with 0.3% TDI or vehicle (2:3 AOO) (20µl) on the dorsum of both ears. On day 14, 40 µl NP suspensions (0.8 mg/kg TiO_2 and Au) or 2.5 mM trisodium citrate (vehicle) were given through oropharyngeal aspiration under light isoflorane anesthesia. On day 15, the mice were challenged oropharyngeally with 0.01% TDI as described previously [33]. On day 16, methacholine provocation was performed, with the collection of BAL, blood and lung tissue for histology.

Experimental groups are designated as AOO/Veh/TDI, TDI/Veh/TDI, AOO/ TiO_2/TDI, TDI/ TiO_2/TDI, AOO/Au/TDI, TDI/Au/TDI. The first abbreviation indicates the agent used for dermal application on days 1 and 8 (AOO: acetone/olive oil; TDI: toluene diisocyanate), the second abbreviation indicates type of NP/vehicle exposure on day 14 (oropharyngeal route) and third abbreviation indicates the TDI-challenge on day 15 (oropharyngeal route).

Airway hyperreactivity (AHR)

Airway hyperreactivity (AHR) to methacholine was assessed 22h after the TDI-challenge, using a forced oscillation technique (FlexiVent, SCIREQ, Montreal, Canada). As previously described, airway resistance (R) and compliance (C) was measured using a "snapshot" protocol. For each mouse, R and C was plotted against methacholine concentration (from 0 to 10 mg/ml) and the AUC was calculated [34].

Bronchoalveolar lavage (BAL):
Cell Counts

On day 16 (22 h after the TDI-challenge – directly after the AHR), the mice were sacrificed by an overdose (90 mg/kg, ip) of pentobarbital, blood was sampled from the retro-orbital plexus and a bronchoalveolar lavage (BAL) was performed, as explained previously [33]. Total and differential cell counts were performed and the BAL supernatant was frozen (-80°C) until further

Endocytosis estimation

To estimate the extent of the phagocytosis of the particle at least 200 macrophages were randomly counted for the microscopically visible presence or absence of NP aggregates inside the cytoplasm at 1000x.

Electron microscopy/microanalysis

Cytospin slides were rinsed in xylene, to remove immersion oil, and embedded using an inverted gelatin capsule of Taab epoxy resin (Taab Laboratories Equipment Ltd., Aldermaston, UK). The polymerized block was removed from the slide and sectioned. Ultrathin sections from BAL of mice exposed to gold particles were mounted on titanium grids and sections from control and titanium dioxide-exposed animals were mounted on copper grids. All sections were examined using a Megaview 3 digital camera and iTEM software (Olympus Soft Imaging Solutions GmbH, Münster, Germany) in a Jeol 100-CXII electron microscope (Jeol UK Ltd., Welwyn Garden City, UK) equipped with a PCXA-1186 energy-dispersive X-ray spectrometer (Link Analytical Ltd., High Wycombe, UK).

Cytokine Analysis

Levels of matrix metallopeptidase-9 (MMP-9), macrophage inflammatory protein-2 (MIP-2) (R&D Systems, Abingdon, UK), tumor necrosis factor alpha (TNF-α), monocyte chemotactic protein-1 (MCP-1), and IL-6 (Invitrogen SA, Merelbeke, Belgium) were measured in undiluted BAL fluid by a sandwich enzyme-linked immunosorbent assay (ELISA), according to the manufacturer's instructions Lower limits of detection were 0.007 ng/ml, 1.5pg/ml, 3 pg/ml, 9 pg/ml, and 3 pg/ml, respectively.

Histological Lesion Scoring

After collection of BAL fluid, lungs were filled in situ with 4% formaldehyde until full inflation of all lobes, as judged visually. Blind scoring for lung injury was done by an experienced pathologist, based on the presence of oedema, infiltrates of

macrophages and neutrophils, and epithelial damage, on hematoxyline and eosin (H&E) stained slides.

Total Serum IgE

Total serum IgE concentration was measured by OptEIA™ Mouse IgE set (Pharmingen; BD Biosciences, Erembodegem, Belgium) after 1/70 dilution according to the manufacturer's recommendations.

Statistical Analysis

Data are shown as means and standard deviations (SD), except for the Area Under the Curve (AUC) data of the AHR, which is shown as mouse individual data and group means. All groups were tested for normality using the Kolmogorov-Smirnov normality test. Additionally, the larger TDI-groups (n=8-9) were tested using the D'Agostino and Pearson omnibus normality test and the Shapiro-Wilk normality test. Since our data were normally distributed, we applied an analysis of variance (ANOVA) followed by Bonferroni test for multiple comparisons using Graphpad (Graphpad Prism 4.01, Graphpad Software Inc, San Diego, USA). A level of $p < 0.05$ (two-tailed) was considered significant.

Results

NP Characteristics

NPs were thoroughly characterized before use, which we described previously [28;31]. The zeta potentials for Au and TiO_2 NPs in 2.5 mM trisodium citrate were -74 and -52 mV, respectively, showing that electrostatic repulsions may be an important factor in stabilizing the suspensions. These large negative zeta potentials of the particles in comparison with zeta potentials in water (data not shown) demonstrate the stabilizing effect of the citrate solution, particularly towards the gold NPs. Analysis of homogeneous suspensions of the nanoparticles in a 2.5 mM trisodium citrate solution by dynamic light scattering showed a single population of 40 nm gold particles and two populations in the TiO_2 samples. Primary TiO_2 particles with a hydrodynamic diameter of 22 nm were detected next to agglomerates or aggregates with a mean hydrodynamic diameter of 272 nm (Fig. 1). On number basis, < 0.01% of the particles were agglomerates or aggregates. On mass basis, 23.8% of the mass was in agglomerates or aggregates. We can conclude that the majority of TiO_2 particles exist as isolated primary particles in the suspension.

Airway Hyperreactivity (AHR)

Figures 2A (resistance) and 2C (compliance) show the airway responsiveness to methacholine measured 22 h after the TDI-challenge (day 16). The mean area under curve (AUC) of each group is depicted in fig 2B and 2D, for resistance and compliance, respectively. There were no differences between the six non-sensitized groups. All TDI-sensitized and TDI-challenged groups (TDI/Veh/TDI; TDI/TiO$_2$/TDI and TDI/Au/TDI) were significantly increased compared to the complete control group (AOO/Veh/AOO). When comparing of TDI-sensitized and challenged mice, only Au NPs exposed mice (TDI/Au/TDI) showed increased AHR (resistance, but not compliance) compared to the TDI/Veh/TDI group.

Bronchoalveolar lavage (BAL)

Total cell counts are presented in Figure 3A. TDI-sensitized, challenged and NP exposed mice (TDI/TiO$_2$/TDI and TDI/Au/TDI) showed a significantly higher total BAL cell count as compared to the complete control groups (AOO/Veh/AOO). TDI-sensitized and TDI-challenged mice with NP (both TiO$_2$ and Au) exposure showed a

significantly higher inflammation as compared to TDI-sensitized mice without NP exposure. Total macrophage counts are presented in Figure 3B and show the same trends and significant differences as the total BAL cell count. Total neutrophil and eosinophil counts are presented in Figure 3C and D, respectively. TDI-sensitization and challenge led to significant influx of neutrophils and eosinophils in BAL compared to the complete control group. . NP exposed TDI-sensitized and challenged mice had significantly higher neutrophil, but not eosinophil, counts compared to the TDI/Veh/TDI group.

Table 1 shows the average levels of BAL cytokines. We found significant increased levels of MMP-9 in all TDI-sensitized and challenged mice, compare to the complete control group. MIP-2 levels were only increased in the NP exposed TDI-sensitized and challenged mice. TNF-α levels were increased in the NP exposed non-sensitized, but TDI-challenged groups, compared to the AOO/Veh/AOO group. On the other hand, the level of TNF-α in the TDI/Au/TDI group was significantly decreased compared to the TDI/Veh/TDI group. IL-6 was significantly decreased in the TDI/Au/TDI group compared to the AOO/Veh/AOO group. Levels of MCP-1 were similar in all groups.

In figure 4A representative images of BAL macrophages in the TDI-sensitized and challenged mice, with or without NP exposure are shown. Figure 4B shows the percent macrophages which have taken up NPs. In the groups not exposed to NPs no macrophages with NPs were found, therefore, these groups were not included in the statistical analysis. Both in the TiO_2 and in the Au exposed groups, significant differences are found between the non-sensitized and the TDI-sensitized and TDI-challenged mice. We also find a significantly higher percent of macrophages with TiO_2 uptake compared to Au uptake in the non-sensitized, but TDI-challenged control group (AOO/TiO_2/TDI vs AOO/Au/TDI).

Clusters of electron-dense particles were evident in the cytoplasm of macrophages in cytospin preparations from mice exposed to either gold or titanium dioxide nanoparticles (Fig. 4C-D). The composition of these particles was established by microanalysis (Fig. 4E-F). No particle clusters were found in control samples.

Histological Lesion scoring

Figure 5 shows images of H&E stained lungs (50x and 400x) and an histological scoring of the different groups is shown in figure 6. The complete control

group, AOO/Veh/AOO, did not show any signs of oedema, epithelial damage, nor macrophage or neutrophil inflammation, perivascular or peribronchial. Since the semi-quantitative score for the AOO/Veh/AOO group was 0 overall, we could not perform statistics compared to this complete control group. The lungs of the TDI/Veh/TDI group show a slight neutrophilic inflammation, along with oedema and limited epithelial damage. The lungs of the TDI/TiO$_2$/TDI show significantly more macrophage infiltration compared with the TDI/Veh/TDI group, while the TDI/Au/TDI group shows significantly more macrophage and neutrophilic inflammation, along with oedema and epithelial damage, compared to the TDI/Veh/TDI mice.

Total serum IgE

Table 2 shows total serum IgE concentrations. TDI-sensitized and TDI-challenged mice with or without NP exposure have a significantly higher total serum IgE concentrations as compared to their control groups. Further between the TDI-sensitized and challenged groups no difference was measured.

Discussion

A critical look at the available literature emphasizes the need for assessment of NP induced effects in the occupationally exposed/sensitized individuals [14;15;35;36]. Only a few studies investigated the modulation of disease by nanoparticles [37;38]. This is the first study describing the aggravation of both pulmonary function and the inflammation due to NPs exposure in a murine model of diisocyanate-induced occupational asthma; as shown in an increase in airway reactivity, BAL macrophages and neutrophils, along with increased oedema and epithelial damage.

There are no literature reports available on the effects of TiO_2 and Au NPs on AHR alone or in diseased animal models. In our experiments the AHR (increased airway resistance), was only significantly enhanced by Au NPs in sensitized animals. This is in line with particles exposure (carbon black NPs and diesel exhaust particles) in a mouse model of ovalbumin-induced asthma [39;40]. The increased sensitivity to methacholine was probably the result of the increased lung inflammation and the damage of the lung epithelium. Moreover, there was no effect on the compliance of the lungs in response to methacholine provocation, suggesting an influence of the inflammation on the hypersensitivity rather than structural changes of the lung tissue.

Airway inflammation plays a key role in different pathologies including asthma. Some studies have demonstrated that TiO_2 NPs have potential to induce lung inflammation in laboratory animals [26;41;42] but there is no information available for Au NPs. In this study we have used a low dose of NPs, only inducing a minimal pulmonary response. Previously published studies obtained inflammatory response at much higher doses (usually about 5 mg/kg) while we have used only 0.8 mg/kg (approximately 16 µg/mouse). At this particular dose we only found, in NP exposed, non-sensitized animals, a mild cellular inflammatory response, mainly comprised of macrophages, without a significant influx of neutrophils and/or eosinophils. Moreover, the percentage, and therefore also the number, of macrophages in the BAL fluid that were associated with NPs was significantly higher in sensitized animals. EDX analysis of the particles in the macrophages revealed that these were the actual NPs to which the mice were exposed, indicating that the NPs reached the lungs and were

internalized by the macrophages. Also, the control mice that received NPs barely responded to methacholine in resistance and compliance. This indicates that NP exposure without TDI-sensitization, but with TDI-challenge does not induce hypersensitivity, and only limited lung damage.

The current TWA values for a single shift for TiO_2 varies between 15 and 1.5 mg/m³ (*http://www.cdc.gov/niosh/review/public/tio2/pdfs/TIO2Draft.pdf*) *[43].* When we re-calculate the dose used in the mice (0.8 mg/kg), for a human of 70 kg, it is 56 mg. This means that a worker exposed to 6 mg/m³, inhaling averagely 10 m³ per workday is approximately inhaling 60 mg TiO_2. Of course, we are aware that only a fraction of this inhaled dust reaches and remains in the lung, but this illustrates very well that the dose used is relatively realistic. Certainly when taking into account that workers are exposed daily to particles in the air.

Our results demonstrate the aggravation of pulmonary inflammation (both cellular as at the level of cytokine and chemokines production) by NPs even at the low doses used. We observed a 4-fold increase in neutrophil counts in case of sensitized animals exposed to Au and a 2.5-fold increase in sensitized animals exposed to TiO_2 NPs. Studies in ovalbumin asthma model have described the potency of carbon black [38] and diesel exhaust particles to increase the allergen induced pulmonary inflammation [39;40]. A recent study with latex NPs has shown the inability of NPs to increase eosinophilic lung inflammation in the ovalbumin model of asthma [44]. Modulation of OVA induced asthma in mouse model by TDI [45] or bakery flour has also been reported [46]. Particle exposures in the lung leads to macrophage recruitment and during concomitant challenged with TDI a significant augmentation of neutrophilic chemo-attraction is observed. It has been shown that activated alveolar macrophages can lead to the recruitment of neutrophils [47] and macrophage products (MIP-2, CNIC/gro) play a direct role in neutrophil recruitment in infected lungs [48]. Furthermore, it has been shown that macrophages release a neutrophil chemoattractant, macrophage-derived neutrophil chemotactic factor (MNCF), when incubated with LPS, IL-8, TNF-α and INF-γ [49]. In our experiments, we found the highest levels of TNF-α in the non-sensitized, NP exposed and TDI-challenged mice, and not in the NP exposed, TDI-sensitized and TDI-challenged

14

mice, suggesting that other pathways are activated in sensitized mice, compared to non-sensitized mice.

In our study NPs did not affect the IgE levels. Previously in an ovalbumin model of respiratory allergy, modulating effects of ambient air particles, diesel exhaust and wood smoke particles have been observed [50-52]. In our study, the presence of total IgE in serum serves as a good marker of prior sensitization in mice, but has limited functional consequences. This confirms the hypothesis of a non-IgE mediated cellular mechanism involved in the development of chemical-induced asthma.

Histological lesions consisted of perivascular and peribronchial neutrophilic and macrophage infiltration, shedding and necrosis of the epithelium and eodema. Histological lesion scoring further indicated that severity of pathological response in sensitized mice was significantly increased in case of Au NPs exposure. Macrophages readily engulfed these particles, apparent as pigmentation in the histological sections.

The mechanism behind NPs induced modulation of asthma is still unclear. NP induced oxidative damage could be one of the leading factor as oxidative stress plays an important role in the pathogenesis of asthma and we have already shown the abilities of these NPs to produce oxidative stress in cultured bronchial epithelial cells [28;31;53]. Other possible mechanism might be the particle induced epithelial damage to respiratory barrier which leads to increased susceptibility to allergens [54-56]. In line with this, it has also been shown that MMP-9 modulates the tight junction integrity of airway epithelium, thereby initiating lung tissue remodeling [57]. Furthermore, NP also have directly an influence on the maturation, antigen presenting and co-stimulation of antigen presenting cells (APC), as reported by Palomäki et al. [58].

We expected some substantial differences between the two particles, in sensitized mice. The findings are a little counter intuitive because we anticipated that the crystalline TiO_2 particles [59] would induce a more severe inflammatory response compared to the colloid gold which is supposed to be less inflammatory [60].

15

Notwithstanding the significant differences between the two particles in chemistry, physical appearance, size …), both induced a strong influx of inflammatory cells in the lung, a significant increase in MMP-9 and MIP-2, but a relative low pro-inflammatory signal (TNF-α and IL-6) in TDI-sensitized mice. In conclusion, we have demonstrated that both Au NPs aggravate the airway hyperreactivity as well as the inflammatory response in TDI sensitized animals, while TiO_2 NPs only significantly increases the inflammatory response in TDI sensitized animals. These results indicate the possibility of aggravation of chemical induced occupational asthma in the presence of NP exposure. Further studies are warranted to understand the mechanisms underlying this aggravation of asthmatic responses.

Acknowledgements

Tables

Table 1: BAL cytokines

	MMP-9 (ng/ml)	MIP-2 (pg/ml)	MCP-1 (pg/ml)	TNF-α (pg/ml)	IL-6 (pg/ml)
AOO/Veh/AOO	0.14 ± 0.26	9.66 ± 1.91	17.17 ± 7.75	371.0 ± 170.9	220.4 ± 67.1
AOO/Veh/TDI	1.59 ± 1.21	12.90 ± 1.64	25.67 ± 11.39	811.9 ± 415.0	260.1 ± 116.0
TDI/Veh/TDI	2.55 ± 2.30 *	15.45 ± 6.74	24.38 ± 8.55	524.3 ± 226.1	136.9 ± 74.8
AOO/TiO$_2$/AOO	0.62 ± 0.43	9.52 ± 0.67	15.71 ± 8.28	360.5 ± 129.4	206.2 ± 63.7
AOO/TiO$_2$/TDI	1.81 ± 2.06	10.62 ± 2.14	26.37 ± 13.37	1111.0 ± 649.0 **	265.3 ± 119.4
TDI/TiO$_2$/TDI	3.97 ± 2.31 **	18.65 ± 9.87 *	26.13 ± 9.21	323.0 ± 180.6	135.1 ± 115.6
AOO/Au/AOO	1.34 ± 1.59	10.10 ± 1.29	14.90 ± 4.87	304.2 ± 114.8	307.5 ± 90.8
AOO/Au/TDI	2.68 ± 2.78	13.62 ± 3.85	31.91 ± 11.93	957.2 ± 490.5 *	300.6 ± 114.4
TDI/Au/TDI	4.56 ± 1.57 **	20.25 ± 7.89 **	29.89 ± 17.96	189.8 ± 127.1 [+]	71.4 ± 81.1 *

Concentrations of MMP-9, MIP-2, MCP-1, TNF-α and IL-6 were measured, via standard ELISA, in BAL. Experimental groups are identical to Fig. 2. Data are presented as mean ± S.D. n = 5-9 per group. * $p<0.05$, ** $p<0.01$ compared to the AOO/Veh/AOO group;

+ $p<0.05$ compared to the TDI/Veh/TDI group.

Table 2: Total serum IgE (ng/ml)

	IgE (ng/ml)
AOO/Veh/AOO	272 ± 160
AOO/Veh/TDI	276 ± 174
TDI/Veh/TDI	2359 ± 1703 *
AOO/TiO$_2$/AOO	339 ± 286
AOO/TiO$_2$/TDI	271 ± 255
TDI/TiO$_2$/TDI	2548 ± 2237 *
AOO/Au/AOO	315 ± 193
AOO/Au/TDI	229 ± 140
TDI/Au/TDI	2699 ± 1844 *

Total serum IgE levels were analyzed 24 h after the TDI-challenge. Experimental groups are identical to figure 2. n=5-9. * $p < 0.05$ compared to the AOO/Veh/AOO group.

Legends

Figure 1: Dynamic light scattering analysis of gold and titanium dioxide NPs
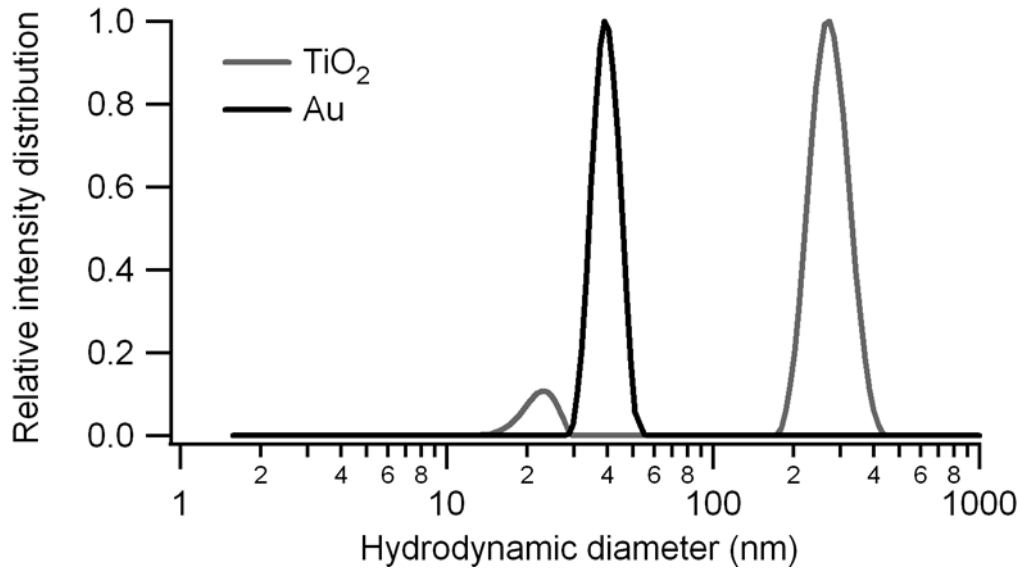
Figure 2: Airway hyperreactivity (AHR).

A) Airway resistance (R) and **B)** compliance (C) to methacholine exposure was measured by forced oscillation technique (FlexiVent) 22 hours after the TDI-challenge. **C)** Area under curve (AUC) of the R and **D)** AUC of C. Experimental groups are AOO/Veh/TDI, TDI/Veh/TDI, AOO/TiO$_2$/TDI, TDI/TiO$_2$/TDI, AOO/Au/TDI, TDI/Au/TDI. The first abbreviation indicates the agent used for dermal application on days 1 and 8 (AOO: acetone/olive oil; TDI: Toluene diisocyanate), the second abbreviation indicates type of NP/vehicle exposure on day 14 (oropharyngeal route) and third abbreviation indicates the TDI-challenge on day 15 (oropharyngeal route). Data are presented as means in fig A and B and as individual values and group means in fig C and D. n=5-9; * p<0.05, ** p<0.01 compared to the AOO/Veh/AOO group; ++ p<0.01 compared to the TDI/Veh/TDI group.

Resistance: AHR
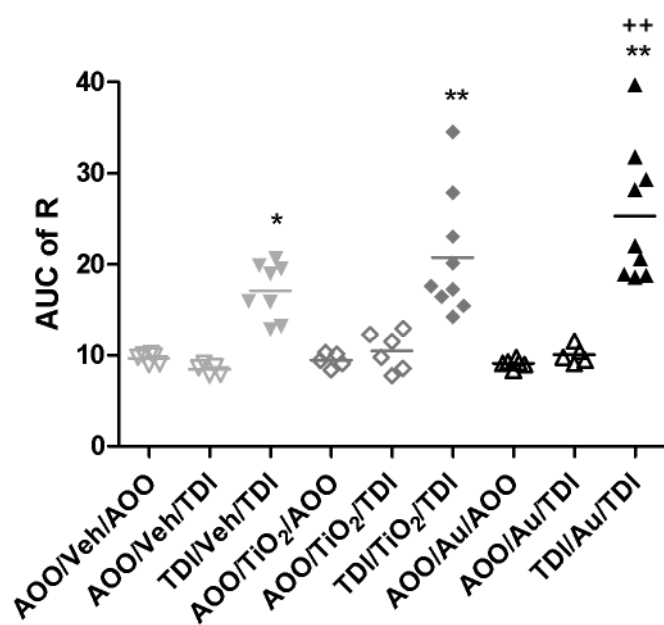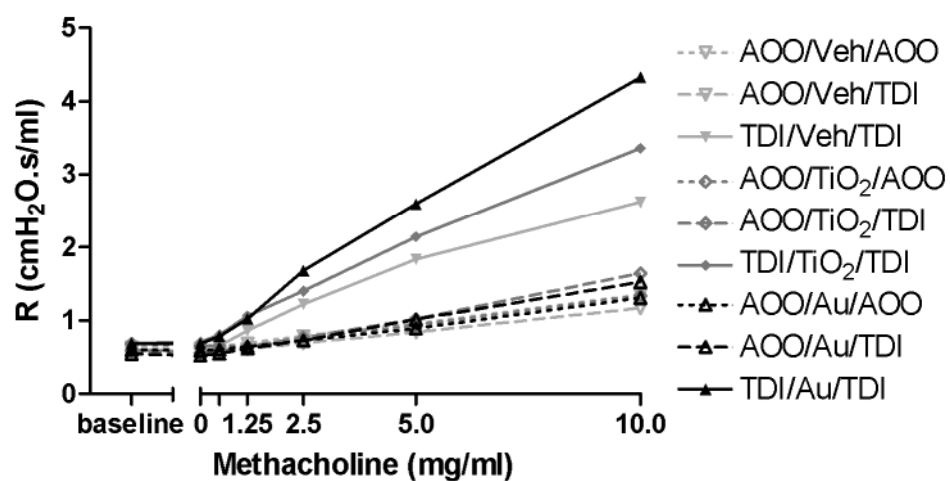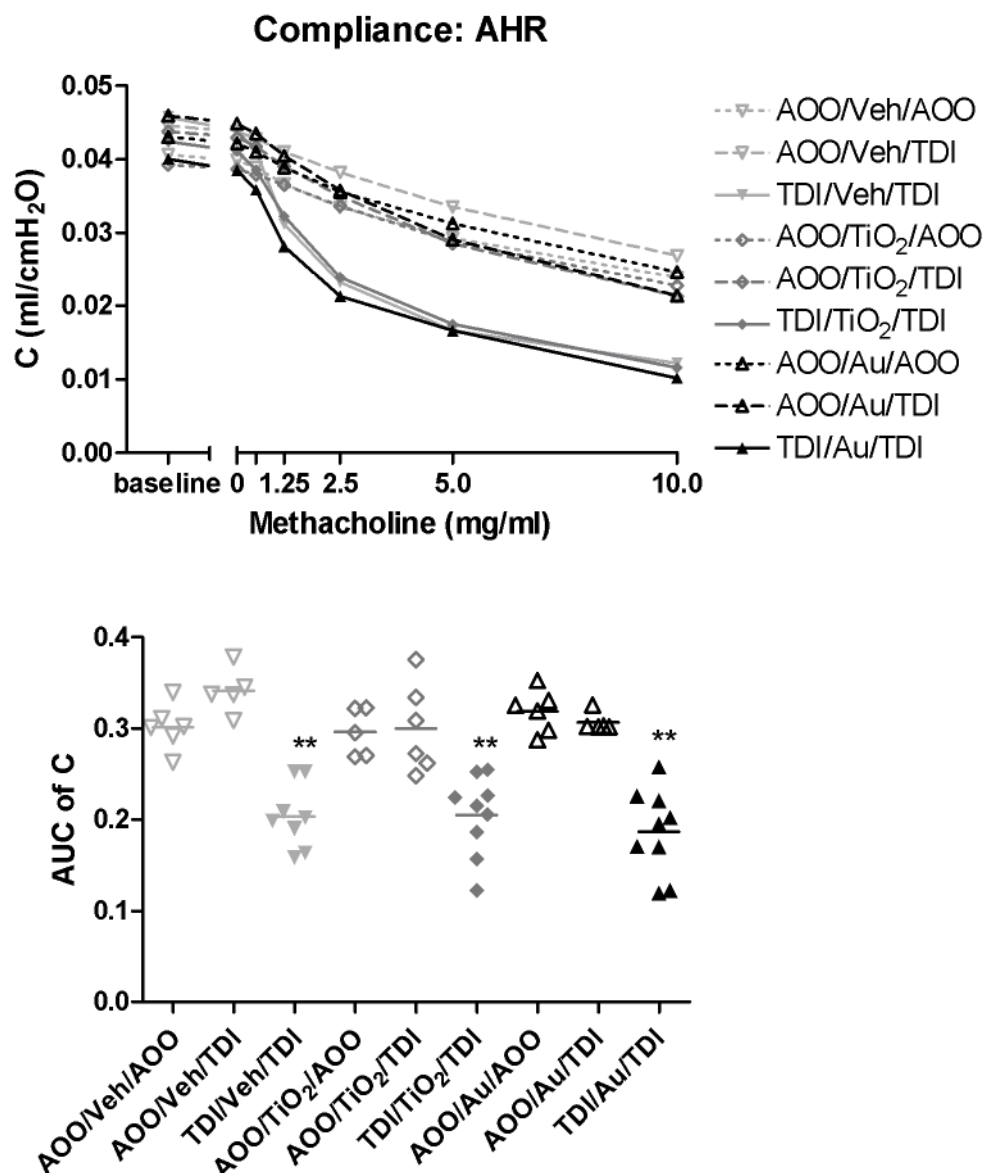
Figure 3: Total and differential BAL cell counts.

BAL fluid was collected 24 h after the TDI-challenge. Experimental groups are identical to figure 1. **A)** BAL total cell count, **B)** BAL total macrophage count, **C)** BAL total neutrophil count, **D)** BAL total eosinophils count. Experimental groups are identical to figure 2. Data are presented as mean ± S.D. n=5-9 per group. * $p < 0.05$, ** $p < 0.01$, *** $p < 0.001$ compared to the AOO/Veh/AOO group; +++ $p < 0.001$ compared to the TDI/Veh/TDI group.

BAL Total cell count

BAL macrophages

BAL neutrophils
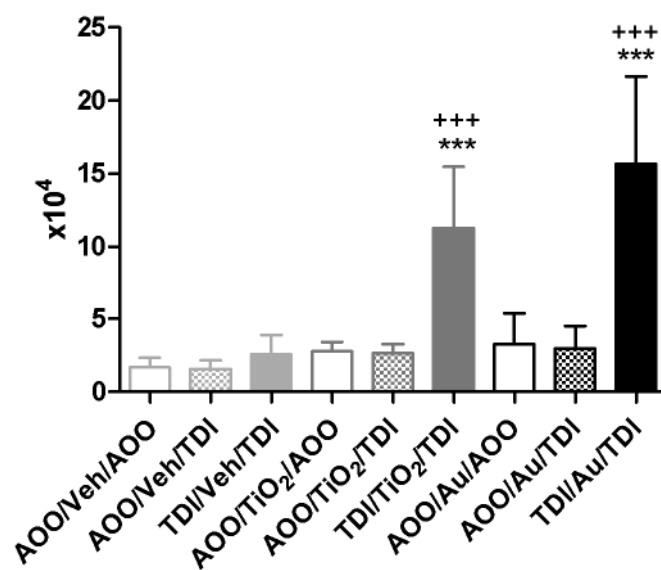
BAL eosinophils
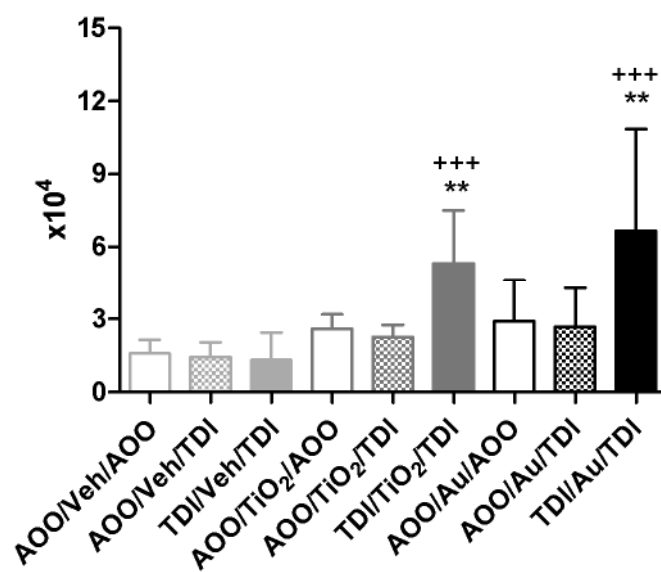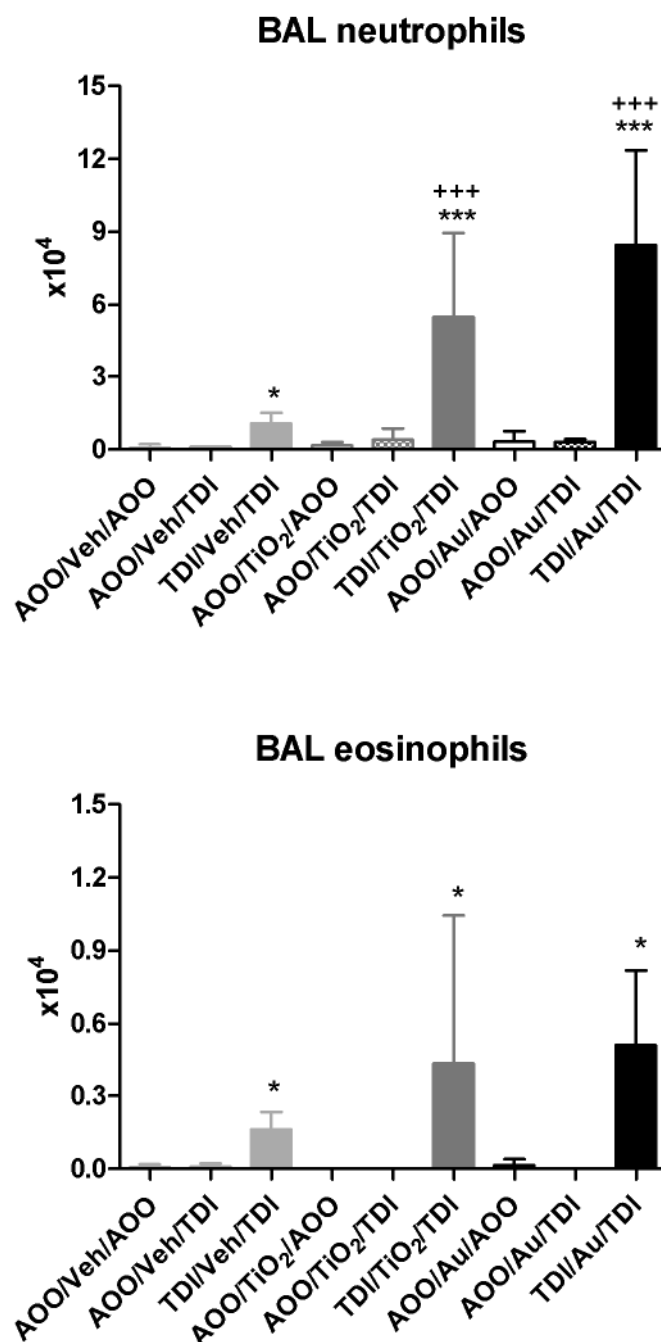
Figure 4: NP uptake by BAL Macrophages and analysis of internalized particles.

A) Representative images of one macrophage from each group. **B)** Percent macrophages with NPs in the cytoplasm. Transmission electron micrograph showing clusters of electron-dense particles, in the cytoplasm of a macrophage from a mouse exposed to gold nanoparticles **(C)** or titanium

dioxide nanoparticles **(D)**. X-ray spectrum from the area indicated in panel A (white circle and arrow) showing the Mα Lα Lβ₁and Lβ₂ peaks for gold together with the Kα and Kβ peaks for titanium (grid) and background peaks for copper and silicon **(E)**. X-ray spectrum from the area indicated in panel B (white circle and arrow) showing the Kα and Kβ peaks for titanium together with the Kα and Kβ peaks for copper (grid) **(F)**. Experimental groups are identical to figure 2. Magnification 1000x; n=5-6; *** p<0.001.
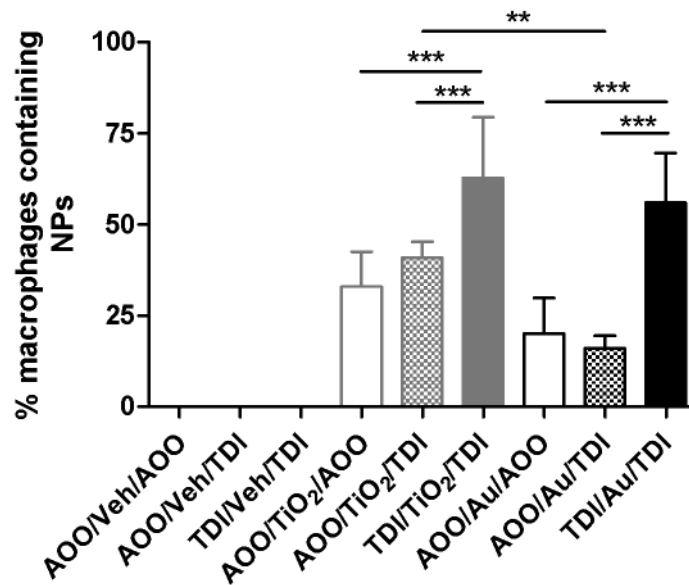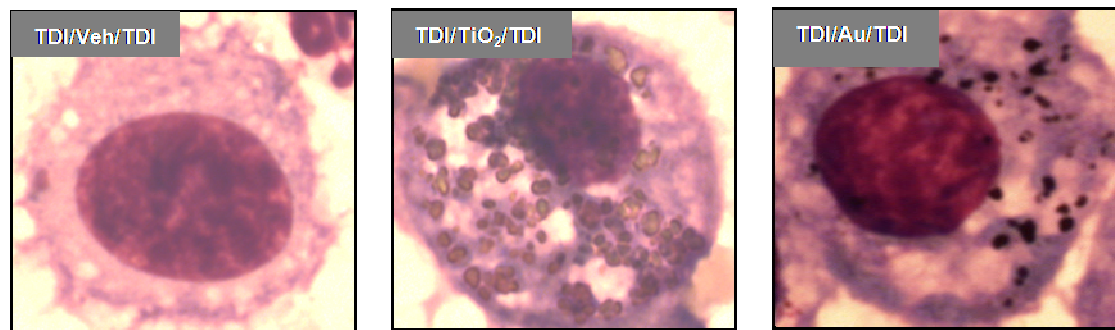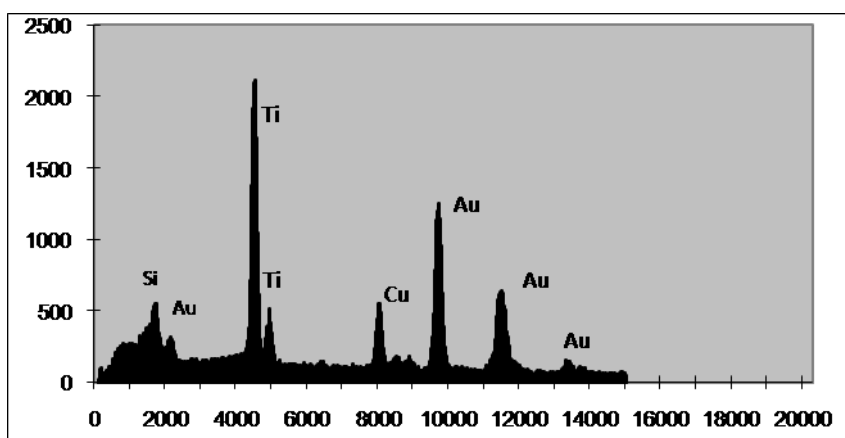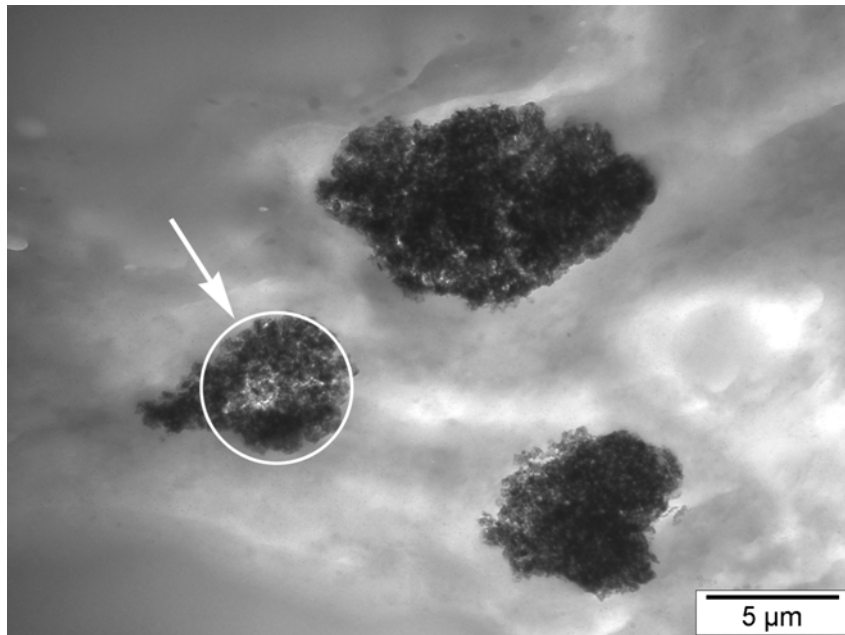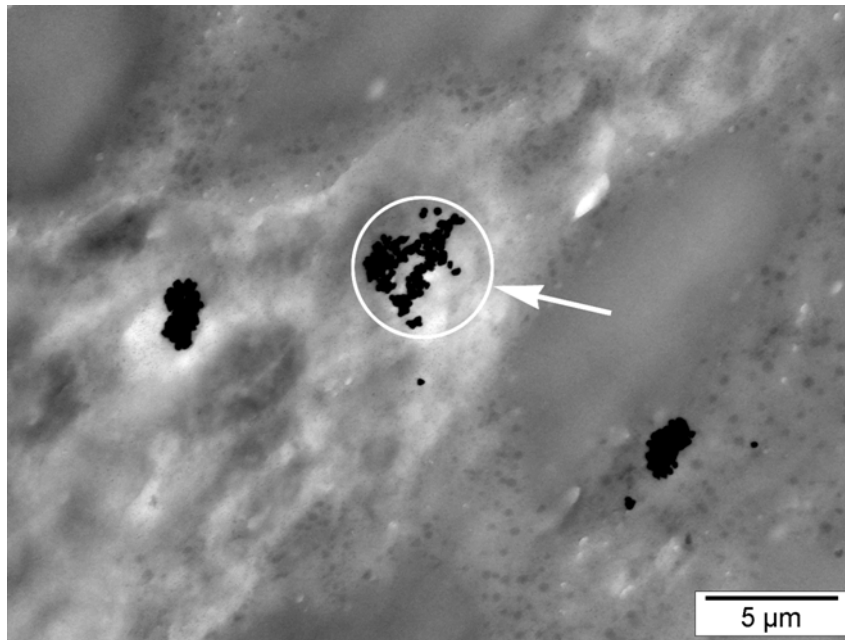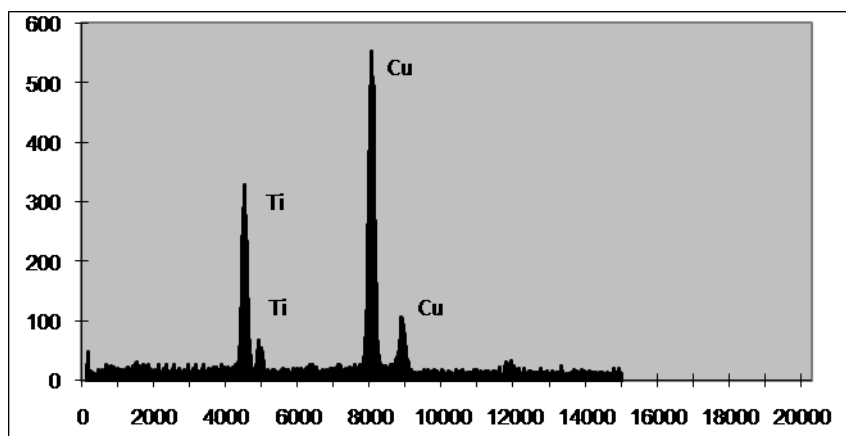
Figure 5: Histological analysis of lung tissue.

Lungs were isolated and fixed with formaldehyde. Semi fine sections were cut after paraffin embedding. Slide were stained with H&E staining and analyzed for pathological lesions. Magnification of 50x and 400x are presented. Experimental groups are identical to figure 2.
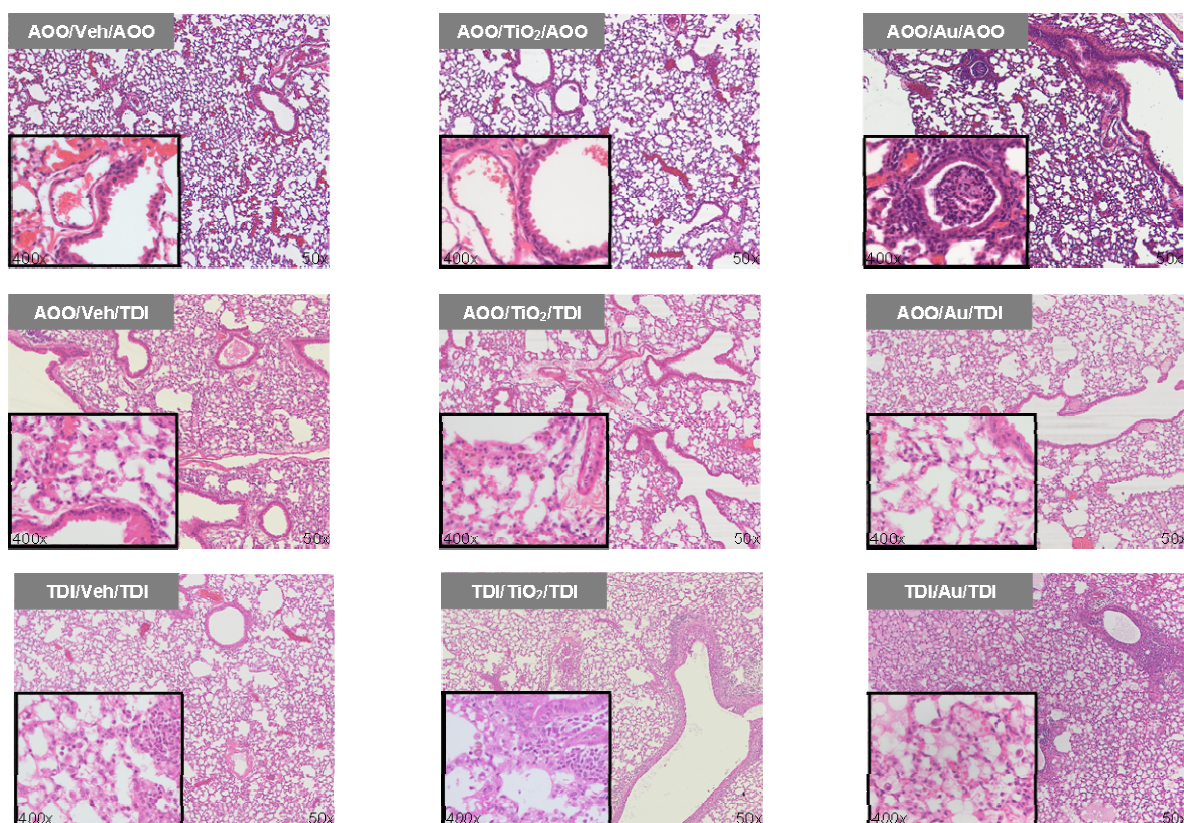
Figure 6: Semi-quantitative scoring of lung histology.

Lungs were isolated and fixed with formaldehyde. Semi fine sections were cut after paraffin embedding. Slide were stained with H&E staining and analyzed for pathological lesions. A semi-quantitative scoring, ranging from 0 (nothing) to 3 (substantial) of the lungs was performed in a blinded manner. **A)** eodema accumulation, **B)** epithelial damage, **C)** macrophage infiltration, **D)** neutrophil infiltration. Experimental groups are identical to figure 2. n=5-9. + $p<0.05$, ++ $p<0.01$ +++ $p<0.001$ compared to the TDI/Veh/TDI group.

Oedema

Epithelial damage
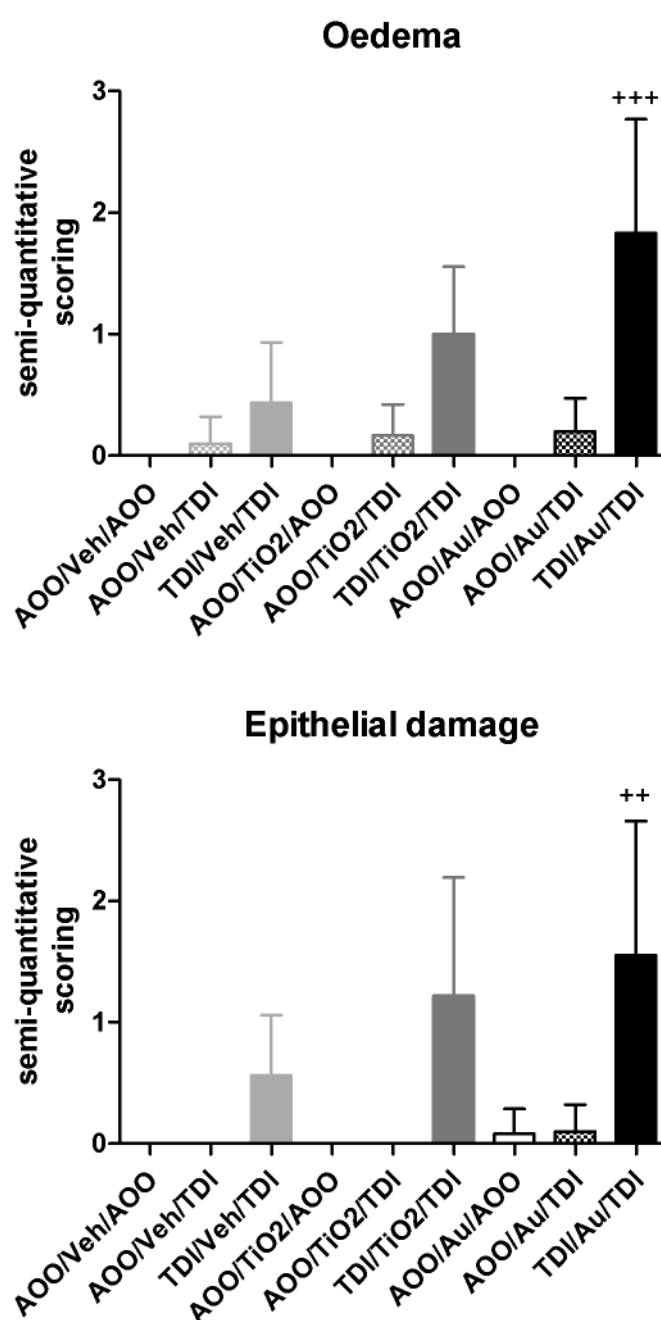
Macrophage infiltration
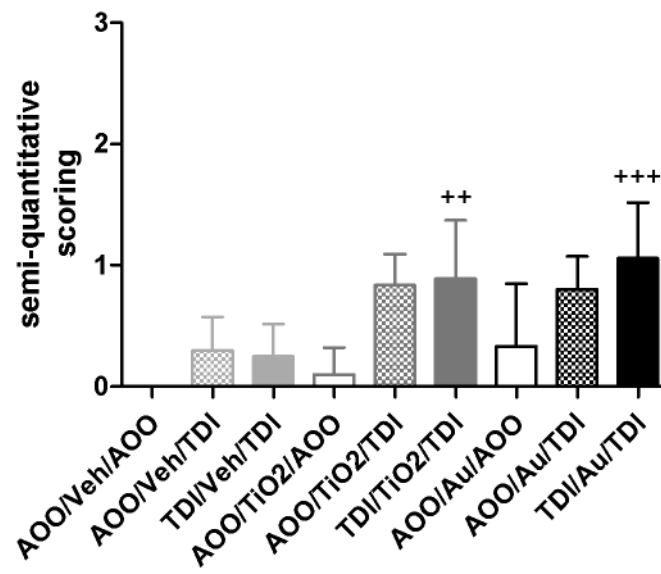
Neutrophil infiltration
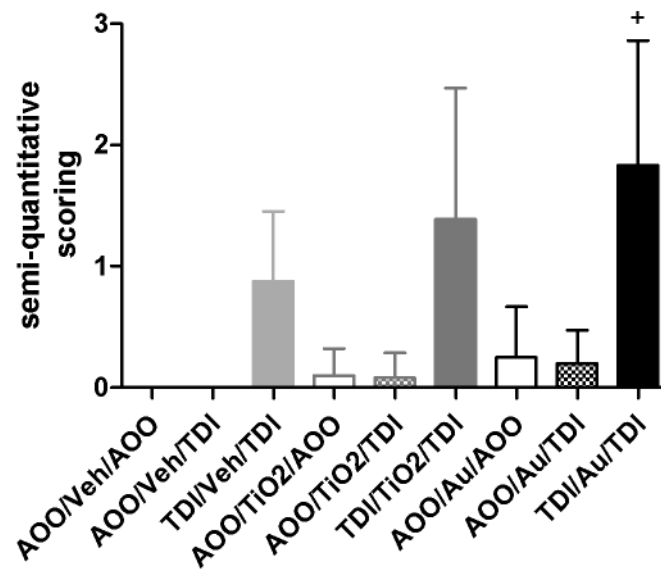
References

1. Malo JL, Lemiere C, Gautrin D, Labrecque M. Occupational asthma. *Curr Opin Pulm Med* 2004; 10(1): 57-61.

2. Boulet LP, Lemiere C, Gautrin D, Cartier A. New insights into occupational asthma. *Curr Opin Allergy Clin Immunol* 2007; 7(1): 96-101.

3. Bello D, Herrick CA, Smith TJ, Woskie SR, Streicher RP, Cullen MR, Liu Y, Redlich CA. Skin exposure to isocyanates: reasons for concern. *Environ Health Perspect* 2007; 115(3): 328-35.

4. Vanoirbeek JA, Tarkowski M, Ceuppens JL, Verbeken EK, Nemery B, Hoet PH. Respiratory response to toluene diisocyanate depends on prior frequency and concentration of dermal sensitization in mice. *Toxicol Sci* 2004; 80(2): 310-21.

5. Tarkowski M, Vanoirbeek JA, Vanhooren HM, De V, V, Mercier CM, Ceuppens J, Nemery B, Hoet PH. Immunological determinants of ventilatory changes induced in mice by dermal sensitization and respiratory challenge with toluene diisocyanate. *Am J Physiol Lung Cell Mol Physiol* 2007; 292(1): L207-L214.

6. Vanoirbeek JA, De V, V, Vanhooren HM, Nawrot TS, Nemery B, Hoet PH. How long do the systemic and ventilatory responses to toluene diisocyanate persist in dermally sensitized mice? *J Allergy Clin Immunol* 2008; 121(2): 456-63.

7. Redlich CA, Herrick CA. Lung/skin connections in occupational lung disease. *Curr Opin Allergy Clin Immunol* 2008; 8(2): 115-9.

8. Petsonk EL, Wang ML, Lewis DM, Siegel PD, Husberg BJ. Asthma-like symptoms in wood product plant workers exposed to methylene diphenyl diisocyanate. *Chest* 2000; 118(4): 1183-93.

9. Pronk A, Preller L, Raulf-Heimsoth M, Jonkers IC, Lammers JW, Wouters IM, Doekes G, Wisnewski AV, Heederik D. Respiratory symptoms, sensitization, and exposure response relationships in spray painters exposed to isocyanates. *Am J Respir Crit Care Med* 2007; 176(11): 1090-7.

10. Ban M, Morel G, Langonne I, Huguet N, Pepin E, Binet S. TDI can induce respiratory allergy with Th2-dominated response in mice. *Toxicology* 2006; 218(1): 39-47.

11. Herrick CA, Das J, Xu L, Wisnewski AV, Redlich CA, Bottomly K. Differential roles for CD4 and CD8 T cells after diisocyanate sensitization: genetic control of TH2-induced lung inflammation. *J Allergy Clin Immunol* 2003; 111(5): 1087-94.

12. De Vooght V, Cruz MJ, Haenen S, Wijnhoven K, Munoz X, Hoet PH, et al. Ammonium persulfate can initiate an asthmatic response in mice. Thorax. In press 2010.

13. Woodrow Wilson Database. http://www.nanotechproject.org. Date last updated: August 2009, Date last accessed: October 2009. 2009.

14. Song Y, Li X, Du X. Exposure to nanoparticles is related to pleural effusion, pulmonary fibrosis and granuloma. *Eur Respir J* 2009; 34(3): 559-67.

15. Gilbert N. Nanoparticle safety in doubt. *Nature* 2009; 460(7258): 937.

16. Xia T, Kovochich M, Brant J, Hotze M, Sempf J, Oberley T, Sioutas C, Yeh JI, Wiesner MR, Nel AE. Comparison of the abilities of ambient and manufactured nanoparticles to induce cellular toxicity according to an oxidative stress paradigm. *Nano Lett* 2006; 6(8): 1794-807.

17. Kaida T, Kobayashi K, Adachi M, Suzuki F. Optical characteristics of titanium oxide interference film and the film laminated with oxides and their applications for cosmetics. *J Cosmet Sci* 2004; 55(2): 219-20.

18. Long TC, Tajuba J, Sama P, Saleh N, Swartz C, Parker J, Hester S, Lowry GV, Veronesi B. Nanosize titanium dioxide stimulates reactive oxygen species in brain microglia and damages neurons in vitro. *Environ Health Perspect* 2007; 115(11): 1631-7.

19. Sperling RA, Rivera GP, Zhang F, Zanella M, Parak WJ. Biological applications of gold nanoparticles. *Chem Soc Rev* 2008; 37(9): 1896-908.

20. Ghosh P, Han G, De M, Kim CK, Rotello VM. Gold nanoparticles in delivery applications. *Adv Drug Deliv Rev* 2008; 60(11): 1307-15.

21. De Wall SL, Painter C, Stone JD, Bandaranayake R, Wiley DC, Mitchison TJ, Stern LJ, Decker BS. Noble metals strip peptides from class II MHC proteins. *Nat Chem Biol* 2006; 2(4): 197-201.

22. Cheng Y, Samia C, Meyers JD, Panagopoulos I, Fei B, Burda C. Highly efficient drug delivery with gold nanoparticle vectors for in vivo photodynamic therapy of cancer. *J Am Chem Soc* 2008; 130(32): 10643-7.

23. Novelli F, Recine M, Sparatore F, Juliano C. Gold(I) complexes as antimicrobial agents. *Farmaco* 1999; 54(4): 232-6.

24. Frampton MW, Utell MJ, Zareba W, Oberdorster G, Cox C, Huang LS, Morrow PE, Lee FE, Chalupa D, Frasier LM, Speers DM, Stewart J. Effects of exposure to ultrafine carbon particles in healthy subjects and subjects with asthma. *Res Rep Health Eff Inst* 2004; (126): 1-47.

25. von Klot S., Wolke G, Tuch T, Heinrich J, Dockery DW, Schwartz J, Kreyling WG, Wichmann HE, Peters A. Increased asthma medication use in association with ambient fine and ultrafine particles. *Eur Respir J* 2002; 20(3): 691-702.

26. Warheit DB, Webb TR, Sayes CM, Colvin VL, Reed KL. Pulmonary instillation studies with nanoscale TiO2 rods and dots in rats: toxicity is not dependent upon particle size and surface area. *Toxicol Sci* 2006; 91(1): 227-36.

27. Sayes CM, Reed KL, Warheit DB. Assessing toxicity of fine and nanoparticles: comparing in vitro measurements to in vivo pulmonary toxicity profiles. *Toxicol Sci* 2007; 97(1): 163-80.

28. Hussain S, Boland S, Baeza-Squiban A, Hamel R, Thomassen LC, Martens JA, Billon-Galland MA, Fleury-Feith J, Moisan F, Pairon JC, Marano F. Oxidative stress and proinflammatory effects of carbon black and titanium dioxide nanoparticles: role of particle surface area and internalized amount. *Toxicology* 2009; 260(1-3): 142-9.

29. Val S, Hussain S, Boland S, Hamel R, Baeza-Squiban A, Marano F. Carbon black and titanium dioxide nanoparticles induce pro-inflammatory responses in bronchial epithelial cells: Need for multiparametric evaluation due to adsorption artifacts. *Inhal Toxicol* 2009; 21(S1): 115-22.

30. Karlsson HL, Gustafsson J, Cronholm P, Moller L. Size-dependent toxicity of metal oxide particles--a comparison between nano- and micrometer size. *Toxicol Lett* 2009; 188(2): 112-8.

31. Hussain S, Thomassen LC, Ferecatu I, Borot MC, Andreau K, Martens JA, Fleury J, Baeza-Squiban A, Marano F, Boland S. Carbon black and titanium dioxide nanoparticles elicit distinct apoptotic pathways in bronchial epithelial cells. *Part Fibre Toxicol* 2010; 7(1): 10.

32. Berne BJ, Pecora R. Dynamic light scattering with applications to chemistry, biology, and physics. New York: Wiley; 1976.

33. De Vooght V, Vanoirbeek JA, Haenen S, Verbeken E, Nemery B, Hoet PH. Oropharyngeal aspiration: an alternative route for challenging in a mouse model of chemical-induced asthma. *Toxicology* 2009; 259(1-2): 84-9.

34. Vanoirbeek JA, Rinaldi M, De V, V, Haenen S, Bobic S, Gayan-Ramirez G, Hoet PH, Verbeken E, Decramer M, Nemery B, Janssens W. Noninvasive and Invasive Pulmonary Function in Mouse Models of Obstructive and Restrictive Respiratory Diseases. *Am J Respir Cell Mol Biol* 2009; 42: 96-104.

35. Kahru A, Savolainen K. Potential hazard of nanoparticles: from properties to biological and environmental effects. *Toxicology* 2010; 269(2-3): 89-91.

36. Savolainen K, Alenius H, Norppa H, Pylkkanen L, Tuomi T, Kasper G. Risk assessment of engineered nanomaterials and nanotechnologies--a review. *Toxicology* 2010; 269(2-3): 92-104.

37. Larsen ST, Roursgaard M, Jensen KA, Nielsen GD. Nano titanium dioxide particles promote allergic sensitization and lung inflammation in mice. *Basic Clin Pharmacol Toxicol* 2010; 106(2): 114-7.

38. Alessandrini F, Schulz H, Takenaka S, Lentner B, Karg E, Behrendt H, Jakob T. Effects of ultrafine carbon particle inhalation on allergic inflammation of the lung. *J Allergy Clin Immunol* 2006; 117(4): 824-30.

39. Inoue K, Takano H, Yanagisawa R, Sakurai M, Abe S, Yoshino S, Yamaki K, Yoshikawa T. Effects of nanoparticles on lung physiology in the presence or absence of antigen. *Int J Immunopathol Pharmacol* 2007; 20(4): 737-44.

40. Takano H, Ichinose T, Miyabara Y, Shibuya T, Lim HB, Yoshikawa T, Sagai M. Inhalation of diesel exhaust enhances allergen-related eosinophil recruitment and airway hyperresponsiveness in mice. *Toxicol Appl Pharmacol* 1998; 150(2): 328-37.

41. Park EJ, Yoon J, Choi K, Yi J, Park K. Induction of chronic inflammation in mice treated with titanium dioxide nanoparticles by intratracheal instillation. *Toxicology* 2009; 260(1-3): 37-46.

42. van Ravenzwaay B., Landsiedel R, Fabian E, Burkhardt S, Strauss V, Ma-Hock L. Comparing fate and effects of three particles of different surface properties: nano-TiO(2), pigmentary TiO(2) and quartz. *Toxicol Lett* 2009; 186(3): 152-9.

43. NIOSH. Evaluation of Health Hazard and Recommandations for Occupational Exposure to Titanium Dioxide. 2005 Nov 22.

44. Inoue K, Takano H, Yanagisawa R, Koike E, Shimada A. Size effects of latex nanomaterials on lung inflammation in mice. *Toxicol Appl Pharmacol* 2009; 234(1): 68-76.

45. Ban M, Langonne I, Huguet N, Pepin E, Morel G. Inhaled chemicals may enhance allergic airway inflammation in ovalbumin-sensitised mice. *Toxicology* 2006; 226(2-3): 161-71.

46. Marraccini P, Brass DM, Hollingsworth JW, Maruoka S, Garantziotis S, Schwartz DA. Bakery flour dust exposure causes non-allergic inflammation and enhances allergic airway inflammation in mice. *Clin Exp Allergy* 2008; 38(9): 1526-35.

47. Robbins RA, Russ WD, Thomas KR, Rasmussen JK, Kay HD. Complement component C5 is required for release of alveolar macrophage-derived neutrophil chemotactic activity. *Am Rev Respir Dis* 1987; 135(3): 659-64.

48. Hashimoto S, Pittet JF, Hong K, Folkesson H, Bagby G, Kobzik L, Frevert C, Watanabe K, Tsurufuji S, Wiener-Kronish J. Depletion of alveolar macrophages decreases neutrophil chemotaxis to Pseudomonas airspace infections. *Am J Physiol* 1996; 270(5 Pt 1): L819-L828.

49. Desouza IA, Hyslop S, Franco-Penteado CF, Ribeiro-DaSilva G. Mouse macrophages release a neutrophil chemotactic mediator following stimulation by staphylococcal enterotoxin type A. *Inflamm Res* 2001; 50(4): 206-12.

50. Alberg T, Cassee FR, Groeng EC, Dybing E, Lovik M. Fine ambient particles from various sites in europe exerted a greater IgE adjuvant effect than coarse ambient particles in a mouse model. *J Toxicol Environ Health A* 2009; 72(1): 1-13.

51. Nygaard UC, Samuelsen M, Aase A, Lovik M. The capacity of particles to increase allergic sensitization is predicted by particle number and surface area, not by particle mass. *Toxicol Sci* 2004; 82(2): 515-24.

52. Samuelsen M, Nygaard UC, Lovik M. Allergy adjuvant effect of particles from wood smoke and road traffic. *Toxicology* 2008; 246(2-3): 124-31.

53. Riedl MA, Nel AE. Importance of oxidative stress in the pathogenesis and treatment of asthma. *Curr Opin Allergy Clin Immunol* 2008; 8(1): 49-56.

54. van Zijverden M., Granum B. Adjuvant activity of particulate pollutants in different mouse models. *Toxicology* 2000; 152(1-3): 69-77.

55. Murphy SA, BeruBe KA, Pooley FD, Richards RJ. The response of lung epithelium to well characterised fine particles. *Life Sci* 1998; 62(19): 1789-99.

56. Devalia JL, Rusznak C, Davies RJ. Allergen/irritant interaction--its role in sensitization and allergic disease. *Allergy* 1998; 53(4): 335-45.

57. Vermeer PD, Denker J, Estin M, Moninger TO, Keshavjee S, Karp P, Kline JN, Zabner J. MMP9 modulates tight junction integrity and cell viability in human airway epithelia. *Am J Physiol Lung Cell Mol Physiol* 2009; 296(5): L751-L762.

58. Palomaki J, Karisola P, Pylkkanen L, Savolainen K, Alenius H. Engineered nanomaterials cause cytotoxicity and activation on mouse antigen presenting cells. *Toxicology* 2010; 267(1-3): 125-31.

59. Monteiller C, Tran L, MacNee W, Faux S, Jones A, Miller B, Donaldson K. The pro-inflammatory effects of low-toxicity low-solubility particles, nanoparticles and fine particles, on epithelial cells in vitro: the role of surface area. *Occup Environ Med* 2007; 64(9): 609-15.

60. Jacobsen NR, Moller P, Jensen KA, Vogel U, Ladefoged O, Loft S, Wallin H. Lung inflammation and genotoxicity following pulmonary exposure to nanoparticles in ApoE-/- mice. *Part Fibre Toxicol* 2009; 6: 2.